

# Holoview: Interactive 3D visualization of medical data in AR

Pankaj Kaushik, Anshul Goswami and Ojaswa Sharma  
Department of Computer Science and Engineering,  
Indraprastha Institute of Information Technology Delhi, India



**Abstract**—We introduce HoloView, an innovative augmented reality (AR) system that enhances interactive learning of human anatomical structures through immersive visualization. Combining advanced rendering techniques with intuitive gesture-based interactions, HoloView provides a comprehensive technical solution for medical education. The system architecture features a distributed rendering pipeline that offloads stereoscopic computations to a remote server, optimizing performance and enabling high-quality visualization on less powerful devices. To prioritize visual quality in the user's direct line of sight while reducing computational load, we implement foveated rendering optimization, enhancing the immersive experience. Additionally, a hybrid surface-volume rendering technique is used to achieve faster rendering speeds without sacrificing visual fidelity. Complemented by a carefully designed user interface and gesture-based interaction system, HoloView allows users to naturally manipulate holographic content and seamlessly navigate the learning environment. HoloView significantly facilitates anatomical structure visualization and promotes an engaging, user-centric learning experience.

**Index Terms**—Article submission, IEEE, IEEEtran, journal, L<sup>A</sup>T<sub>E</sub>X, paper, template, typesetting.

## 1 INTRODUCTION

VIRTUAL Reality (VR) and Augmented Reality (AR) technologies have significantly transformed medical education by introducing innovative tools that transcend the limitations of traditional learning methods. AR headsets, in particular, have emerged as powerful devices in the medical field, providing clinicians and medical students with enhanced insights into patient data and anatomical structures. This paper presents a novel AR application specifically designed to address the growing demand for advanced educational tools, aiming to revolutionize the study of human anatomy for medical students.

In contemporary medical practice, AR applications are widely utilized for diverse purposes, such as anatomy training, patient monitoring, image-guided interventions, and surgical navigation. However, many existing AR systems exhibit notable limitations, particularly in their ability to represent human anatomy comprehensively. These systems [1] [2] often rely on auxiliary tools like desktops with mouse and keyboard setups or large touchscreens for visualization control. While these configurations address visualization challenges, they detract from the immersive experience by requiring additional external devices, which

complicates workflows and burdens users. Furthermore, advancements in AR technology have led to the development of lightweight devices, addressing previous concerns about neck strain or discomfort associated with extended usage.

The AR application introduced in this study is platform-agnostic, capable of being deployed on any AR device without requiring auxiliary tools, thus maintaining a fully immersive experience. Recognizing the computational limitations of AR hardware, the system offloads intensive processing tasks to a remote server, ensuring high performance without compromising device usability. To further enhance the user experience, hand gestures have been incorporated as the primary interaction mechanism, allowing users to interact seamlessly with the system while keeping their hands free for other tasks.

Conventional anatomy learning methods, such as textbooks and videos, provide a foundational understanding but restrict learners to two-dimensional representations, limiting the exploration of anatomical intricacies. By leveraging the Visible Korean Human Project's [3] [4] [5] cryo volume and segmentation data, our AR application introduces a fully immersive, three-dimensional learning environment. This system enables medical students to interact dynamically with anatomical structures and navigate through the human body, even in constrained physical spaces.

The significance of this work lies in its ability to transform anatomy education by offering a highly interactive, engaging, and accessible learning experience. Key contributions of this paper include:

- A comprehensive software system tailored for classroom and clinical environments, providing immersive visualizations, improved depth perception, and user-friendly interactions to support the integration of Mixed Reality (MR) in medical education.
- The introduction of intuitive hand gestures, enabling seamless access, manipulation, and navigation of volumetric medical data without the need for additional devices or controllers.

## 2 RELATED WORK

### 2.1 Volume Rendering

Interactive volume is a sub-domain of volume visualization where users can interact with volume and change

the rendering parameters. One of the pioneering works in this area is the seminal paper by Levoy et al. [6], which introduced the concept of volume rendering using the ray-casting technique. Over time, researchers have explored various approaches to enhance the visual quality and efficiency of volume rendering. Drebin et al. [7] introduced gradient-based shading techniques, such as Phong shading, to improve the perception of surface details within volumetric datasets.

Researchers have investigated advanced rendering techniques incorporating light scattering models to address the challenges posed by volumetric data with complex optical properties. The work by Max et al. [8] proposed a method for simulating light scattering effects in participating media.

To visualize large-scale volumetric datasets, David et al. [9] proposed a hierarchical splatting approach for volume rendering by adaptively refining the level of detail based on the viewing parameters. To visualize features according to the user need, Kindlmann et al. [10] introduced the concept of feature-based transfer functions, enabling users to define volume rendering parameters based on the intrinsic features of the data, such as gradients and curvature.

Advancements in graphics hardware and computational techniques have led to the development of real-time volume rendering methods. The paper by Krüger and Westermann [11] introduced a GPU-based ray-casting algorithm for interactive volume rendering, leveraging the parallel processing power of modern graphics hardware to achieve real-time performance.

As this field grows, researchers try to make the renderer have realistic global lighting effects and have high user interactivity with global rendering parameters. Thomas et al. [12] proposed the interactive photo-realistic renderer in the spirit of having global lighting effects. They use Monte Carlo's estimation technique to estimate the light effects. They were able to simulate the physically based volumetric shadows. In recent works by Siemens [13], they could render hyperrealistic or cinematic images of the CT volume. They incorporated many light interactions with the volume, like sub-surface scattering, multiple scattering, and light-based environment maps.

## 2.2 Augmented Reality in Medical Education

AR technologies have been identified as significant educational tools in medical training. Barsom et al. [14] conducted a systematic review that demonstrated the effectiveness of AR applications in improving medical training outcomes, particularly in surgical procedures and anatomy education. The authors noted that Head-Mounted Displays (HMDs) enable repeated practice without ethical concerns associated with traditional methods, thus facilitating a more engaging learning environment. Barteit et al. [15] emphasized the advantages of AR and Mixed Reality (MR) beyond surgical applications, highlighting their effectiveness in teaching complex subjects like anatomy and anesthesia. Their findings suggest that AR can make intricate medical concepts more accessible, thereby enhancing student comprehension and retention.

Ma et al. [16] introduced a personalized AR system that enables users to visualize anatomical data on their own

bodies, enhancing engagement and understanding. This personalized approach aligns with the findings of Tang et al. [17], who reported that AR technologies improve educational outcomes by providing students with interactive experiences. Additionally, Moro et al. [18] found that three-dimensional visualization methods, including AR, are preferred by students and are more effective than traditional teaching methods in anatomy education.

Additionally, Schott et al. [19] have highlighted how Hololens applications can be used for stereoscopic visualization of 3D data, especially in volumetric medical imaging, providing an improved understanding of three-dimensional structures. Integrating AR with techniques such as cinematic volume rendering emerges as a promising synergy [20], which can revolutionize medical imaging by providing photo-realistic and interactive 3D visualizations of the imaging data. This integration allows for hyper-realistic depictions of deep human anatomy, improving results and elevating the medical training and learning experience.

## 2.3 Navigation in medical volume

Augmented Reality navigation systems have been increasingly integrated into medical procedures, particularly in endoscopy, to enhance navigation and improve patient outcomes. Navigation has been one of the most important innovations in the area of medical examination since the invention of endoscopy. Endoscopy has improved the visualization and diagnosis of the interior of the gastrointestinal structures. Currently, AR navigation systems are only implemented in their early phases because of the difficulty of superimposing multimodal imaging data onto real-time visuals. One of the challenges in AR integration is superimposing multimodal imaging data onto real-time visuals due to organ movement and deformation during procedures [21]. Recent studies [22] have developed AR systems using CT imaging data onto endoscopic views for skull-base surgery, achieving sub-millimeter accuracy, and another that fuses 3D virtual images with real-time endoscopic footage for sinus and skull-base surgery, enhancing surgical safety [23].

Several systems have been created and researched to improve AR navigation visualization in medical volumes. The MD-cave system [1] supports radiologists with immersive 3D viewing and gesture-based interactions but requires extensive hardware setup. SpatialTouch [2] integrated an interactive touch screen for manipulating 3D data with the Hololens, whereas Haowai et al. [24] integrated the 3D slicer tool with the AR for medical data visualization. The VR-RRRoom system [25] offers an immersive 3D environment combining HMDs with interactive surfaces, although its limited touchpoints complicate and limit user interactions and exploration.

Advanced rendering techniques have been employed to improve the realism and interactivity of 3D medical visualizations. Stereoscopic volumetric path tracing has been used to create good interactive stereoscopic visualizations of medical data in VR environments [26]. This approach enhances depth perception and realism compared to traditional 2D medical imaging visualizations while allowing real-time navigation and interaction using VR controllers.

and head tracking. The Multi-Touch Table System for Medical Visualization is another innovative approach, particularly for planning orthopedic surgery [27]. This system provides an intuitive multi-touch interface for visualizing and manipulating 3D medical imaging data. It presents 3D renderings of medical images, enabling surgeons to navigate, manipulate, and annotate the data easily while supporting collaborative viewing and interaction. NextMed [28] is another tool for automatic imaging segmentation, 3D reconstruction, and 3D visualization in AR.

## 2.4 Remote Rendering

Remote rendering, a process involving the generation of 3D graphics on a distant server and subsequent display on a separate device connected through a network, has witnessed notable advancements in addressing challenges related to large-volume visualization and latency reduction. In one of the pioneering works, Bethel et al. [29] developed an early system for visualizing large volumes, storing data on the server, and transmitting only the rendered results to the client, thereby minimizing data transfer. Engel et al. [30] contributed by converting extensive medical volume data into 2D slices for visualization. In contrast, Prohaska et al. [31] proposed a system retrieving only the necessary subvolume from the server, enabling client-side rendering to enhance interaction responsiveness. Shi et al. [32] focused on 3D tele-immersive video, employing depth image rendering and IBR algorithms to mitigate viewpoint change latency. Meanwhile, Schmalstieg [33] suggested utilizing a server as a graphic model database for VR navigation, transmitting only relevant models based on the user’s viewpoint.

Our research explores strategies to ensure high FPS and low latency in the context of dynamic changes in the rendered volume and diverse viewpoints, resembling challenges in cloud gaming. Building upon latency reduction proposals by Eisert and Fichteler [34] and Nave et al. [35], our approach involves compressing and transmitting rendered scenes using TCP. A comprehensive exploration of remote rendering can be found in the survey paper by Shi et al. [36]. Our application’s architecture is very similar to that proposed by Viktor et al. [37].

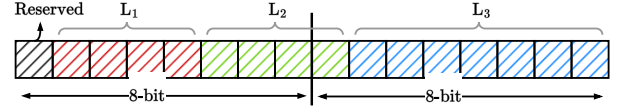
## 3 DATASET PREPARATION

In our application, we use a subset of the Visible Korean Human dataset [3]–[5], which consists of cryosection images of a male cadaver sectioned at intervals of 0.2 mm, resulting in a resolution of  $2468 \times 1407 \times 8506$  of the whole body. We also utilized segmented images of the cryosection data provided for every fifth anatomical image. To extract relevant information for hybrid rendering while minimizing the dataset’s memory footprint, we preprocessed the data as outlined in the following sections.

### 3.1 Representation of segmentation hierarchy

In the Visible Korean Human project, the segmentation data is organized into three hierarchical levels. Level 1 ( $L_1$ ) encompasses 13 human body systems, which are further subdivided into Level 2 ( $L_2$ ) to provide organ-level information. Level 3 ( $L_3$ ) contains detailed segmentation

within each organ. Based on the number of classes in each hierarchical level, we encode this hierarchy into a 16-bit number for every voxel in the segmentation volume. We assign 7 bits starting from the least significant bit (LSB) to  $L_3$ , the next four bits to  $L_2$ , and the subsequent four bits to  $L_1$ , while keeping the the most significant bit (MSB) reserved.



In our work, we only use up to the  $L_2$  level. The background ID is 0 with both  $L_1$  and  $L_2$  bits set to zero.

### 3.2 Correction of mislabeled segments

The segmentation regions in the dataset suffer from issues such as missing labels and incorrect labeling in certain slices. To address major problems with the  $L_1$  and  $L_2$  level segmentation regions, we performed manual inspection and applied semi-automatic techniques. In the manual approach, labels were assigned to unlabeled slices based on the labels of preceding and succeeding slices; manual identification was conducted when neighboring slices had different labels. The semi-automatic approach was used in cases involving multiple consecutive slices of unlabeled regions. In these instances, we applied seeded region growing and level set segmentation methods to segment regions of the missing class.

### 3.3 Homotopy based resampling

The segmentation data is available only for every fifth image of the Cryosection dataset, which poses the problem of losing continuity while visualizing the dataset. In order to upsample the segmentation data we use homotopy continuation based approach [38] for smooth transition of region boundaries between consecutive slices. Specifically, we compute a 2D signed distance field from the segmentation boundaries of each slice and then interpolate this field smoothly for the slices in between. This method effectively upsamples the entire volume, maintaining continuity throughout the dataset. This approach is applied to upsample segmentation regions at both  $L_1$  and  $L_2$  levels, producing two distinct segmentation grids corresponding to each level.

To reduce memory usage, we downsampled the cryosection and segmentation voxel grids to half of their original dimensions, resulting in a resolution of  $1234 \times 703 \times 4253$ .

### 3.4 Mesh creation

During the resampling process, we compute signed distance fields for each segmentation label at the  $L_2$  level, corresponding to individual organs. Surface meshes are then extracted from these signed distance fields and utilized to accelerate our ray-marching-based rendering process. By using these meshes, we optimize rendering by enabling empty space skipping along rays, significantly improving computational efficiency.

Starting with surface meshes extracted using the marching cubes algorithm, we applied decimation to reduce triangle count while preserving overall shape. To address the

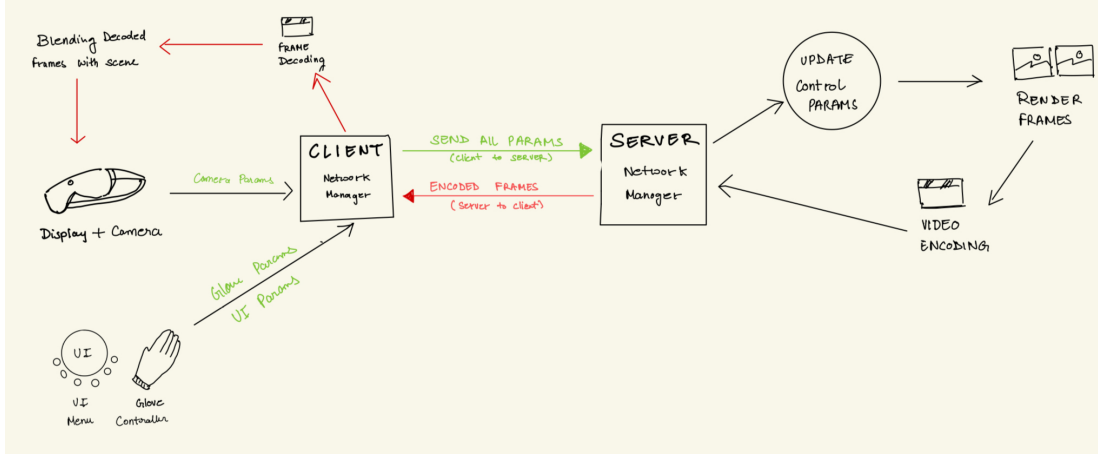


Fig. 1. Overview of our the HoloView system.

roughness introduced by decimation, we used the Taubin smoothing filter [39], which reduces surface irregularities without significant shrinkage. Despite smoothing, high triangle counts remained a concern for efficient rendering. To optimize further, we applied the adaptive remeshing filter of Attene and Falcidieno [40], which reduces triangle density while preserving essential details, ensuring efficient and accurate surface details.

## 4 APPROACH

HoloView is an Augmented Reality (AR) based system that is designed to provide medical students with an intuitive and effective tool for learning anatomy in a seamless and immersive environment. The system utilizes a multi-threaded remote rendering architecture, where real-time stereo rendering of large volumetric datasets is performed on a high-performance server, while the lightweight Microsoft HoloLens AR device functions as a thin client for display. The AR device tracks the user's head and hand orientations along with eye gaze in real-time for an interactive and immersive experience. User interactions, including hand gestures, camera orientation, and rendering parameters, are transmitted to the remote renderer via a *control stream* using the TCP protocol. The renderer generates synchronized stereo frames based on this control data, encodes them, and sends them back to the AR application over a *data stream*. Upon receiving the encoded frames, the application updates the AR device's display in real time. Our design ensures seamless interaction while keeping the user's hands free by eliminating the need for controllers, instead using intuitive hand gestures for all interactions within the AR environment.

HoloView allows users to selectively visualize anatomical structures and gain insights into their functionality or descriptions through intuitive hand gestures. Navigation within confined physical spaces is facilitated through a dual-hand gesture mechanism: the left hand activates the navigation mode, while the right hand determines the camera's movement direction. To explore internal anatomical features, our system enables users to dynamically adjust the visibility of tissues for enhanced visualization. Additionally,

the system integrates a slicing tool by attaching a virtual cutting plane to the user's right hand, allowing precise cross-sectional view of the volume. The integration of advanced interaction methods and optimized rendering in HoloView delivers an immersive and intuitive platform for exploring human anatomy in AR. A detailed overview of the system is provided in Figure 1.

### 4.1 Real-time rendering

The HoloView system uses the Nvidia OptiX ray tracing engine [41] for high-performance GPU rendering and efficient data synchronization. The renderer initializes by loading the Cryosection volume as a set of RGBA CUDA textures and  $L_2$  organ meshes using multi-threaded CPU processing. After initialization, it waits for client connections. Upon connection, a dedicated control stream thread handles client requests, while the main thread remains available for additional connections. Frame requests for the left and right eyes are rendered in parallel using CUDA streams, and stereo frames are transmitted back to the AR application via a separate data stream thread.

#### 4.1.1 Hybrid rendering

In HoloView, we combined surface and volume rendering techniques to optimize the visualization process by leveraging the strengths of both methods. Traditionally a voxel grid is rendered using the raymarching rendering algorithm [?].

that volume rendering typically encloses the volumetric dataset with an axis-aligned bounding box. Rays are cast through each pixel toward this bounding box to determine the start and end points in world space for color accumulation. However, this approach often results in inefficiencies when visualizing a single organ within a complex anatomical dataset. Assigning zero opacity to non-target organ structures creates extensive empty spaces, significantly lowering frame rates.

To address this, we utilize the  $L_2$  meshes (surface-based approximations) to define ray accumulation's start and end points more precisely. By aligning the ray traversal with the boundaries of the selected organ, we eliminate unnecessary computations for irrelevant regions, improving both rendering efficiency and frame rates. The hybrid approach



ensures a balance between the detailed representation of volumetric data and the computational efficiency of surface rendering, providing an optimized solution for interactive medical visualization.

#### 4.1.2 Network optimization

To ensure optimal network performance for our system, we utilized the Wi-Fi router as a dedicated access point. The workstation was connected to the router via an Ethernet cable, while the HoloLens connected wirelessly, forming a local network comprising the HoloLens, the workstation, and the router. We used a 160 MHz band featuring 802.11ax (Wi-Fi 6), HT160, and 1024-QAM, which supports speeds of up to 4803 Mbps. To enhance further connectivity and reduce latency, we enabled beamforming on the router, which focuses the wireless signal towards connected devices for improved stability. Additionally, we minimized physical obstructions in the environment and selected the most efficient communication channel between the workstation and the HoloLens. This configuration ensured a robust and low-latency connection, crucial for real-time AR rendering and interaction.

#### 4.1.3 Foveated rendering

The HoloLens 2 has a native resolution of  $1440 \times 960$ , but transferring rendered stereo images at this resolution reduces the frame rate to approximately 7 fps. In an eye-tracked AR setup, display performance can be improved through foveated rendering, which reduces the number of pixels to be rendered away from the gaze point. To address this, we implemented the foveated encoding method by Ye et al. [42], rendering stereo images at one-third of the resolution in each dimension while maintaining high quality near the gaze point. This approach increases the image transmission rate to 60 fps while preserving visual quality for the user.

### 4.2 Interaction design

Interaction plays an essential role in all imaging and visualization systems. In HoloView, users can interact with and manipulate the holographic representation of the human body (cadaver) to suit their needs. Microsoft Hololens 2 comes without any controllers and uses hand gestures to interact with the holograms. To enhance functionality, we have incorporated additional custom gestures for specific features.

#### 4.2.1 Selection with hand ray

Holoview provides users a virtual mesh representation of the segmentation data from Visible Korean Human data, and to select different organs or body parts, users need to make the pinch gesture by touching the right-hand index tip with the tip of the thumb. The user needs to point at the organ mesh and make the pinch gesture and as feedback, the selected organ will be highlighted with a glowing rim light over the organ. To deselect the organ, the user simply needs to repeat the pinch gesture on the same structure.

#### 4.2.2 UI interactions

The user interface in HoloView is designed and built with the Mixed Reality Toolkit (MRTK) for efficient feature access, shown in Figure 2. The system supports diverse input mechanisms, including hand gestures, and integrates spatially aware UI buttons that blend seamlessly with the physical environment. All UI components are virtually presented, requiring interactions to occur in free air. These buttons provide visual feedback, such as glowing when a user's hand is nearby and highlighting when pointed at, enhancing the naturalness of virtual interactions as if the elements were tangible.

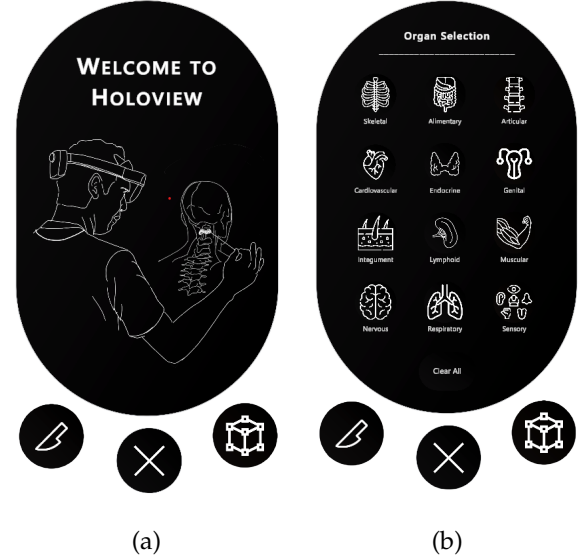


Fig. 2. HoloView interactive UI. (a) Welcome Screen, (b) Organ selection UI.

### 4.3 Slicing Plane

Diagnostic imaging techniques, such as X-rays, CT scans, and MRIs, serve as crucial assessment tools that complement other examinations (physical, neurological, orthopedic, etc.) in arriving at an accurate diagnosis. More often, medical practitioners need to see the cross-section view of the CT or MRI. We have introduced a slicing plane feature to get a cross-section view of the Cryo volume and foster a more immersive exploration of medical data.

To get the slicing plane in the AR world, the User must click the slicing plane button on the UI. A plane will stick to the User's right hand as long as the User keeps his right hand straight and maintains a  $90^\circ$  angle between the fingers and the thumb as shown in figure 3. This functionality empowers users with a slicing plane within the mixed reality world, enabling them to visualize cross-sectional views by slicing through the volume. Users can freely move, rotate, and position the slicing plane as desired. The plane cuts the volume along the user's gaze direction, facilitating intuitive visualization and analysis.

### 4.4 Selective rendering

In the medical field, professionals often require the ability to visualize specific organs rather than the entire human body.

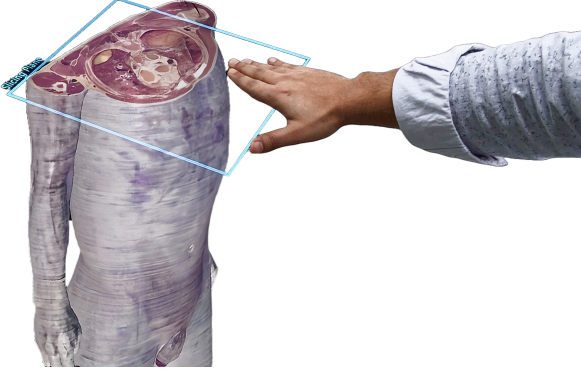


Fig. 3. Image of the sliced Volume using slicing plane to view the cross-section

To cater to this need, we implemented a selective rendering feature that enables users to toggle the visualization of individual organs based on their requirements. Users first select a primary category (Level 1) using the provided UI buttons. Upon selection, the corresponding subcategories (Level 2) organ meshes are displayed as shown in figure 4 with colored meshes. To select a Level 2 organ, users perform a "pinch" gesture with their right hand, achieved by bringing the tips of the index finger and thumb together while pointing to the desired organ. The same gesture can be used to deselect an organ. As feedback, the meshes are highlighted after selection. For added convenience, the interface also includes buttons to "Select All" or "Deselect All" Level 2 organs within a category. The system supports the simultaneous selection of multiple organs, including organs from different Level 1 groups, offering flexibility in visualizations.

One of the challenges in this mode that arises is when the user selects only specific organs of the body to visualize as a hologram, it leads to a lot of empty space inside the volume. Rendering stereo frames with uniform sample steps along the view direction drastically reduces the frame rate, effectively reducing the user's immersion in the virtual world. To overcome this, we used the smoothed meshes of the organs. We have combined the surface and volume rendering. Surfaces were used to find the start and end points for direct volume rendering along the view direction; then, the volume compositing was done from front to back between the start and the endpoint.

To inform the remote renderer about the selected organs, we took advantage of having only 53 sublevels, as shown in Table 1, and represented the selected organs by the user with a 64-bit string. Each L1 is allocated a group of bits corresponding to the number of its sublevels, as specified in Table 1. Each bit within the allocated segment represents a specific sublevel of the corresponding L1 system. A bit value of 1 indicates that the sublevel is selected, while a 0 indicates it is not selected. The bits for each system are concatenated sequentially in the order listed in Table 1, forming the final 53-bit representation as shown in equation 1.

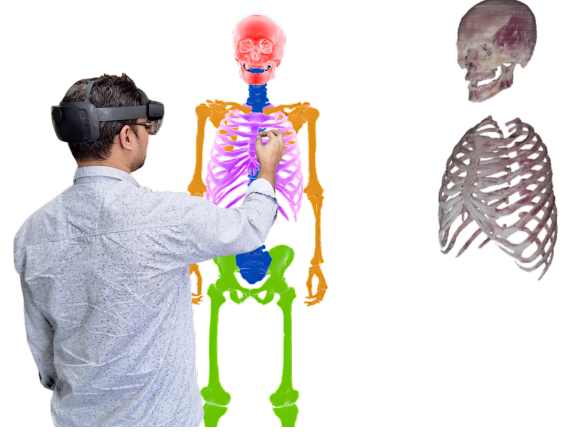


Fig. 4. Shows a user using the Selective rendering feature with the right hand to select an organ by a pinch gesture by pointing to the organ.

System name (L1 label)	Number of Sublevels
Skeletal (1)	5
Lymphoid (2)	1
Nervous (3)	4
Sensory (4)	2
Integument (5)	1
Articular (6)	2
Muscular (7)	7
Alimentary (8)	11
Respiratory (9)	4
Urinary (10)	4
Genital (11)	2
Endocrine (12)	1
Cardiovascular (13)	9
Total (53)	

TABLE 1

Number of sublevels of each L1 system

$$R = \underbrace{\underbrace{X}_{\text{Cardiovascular (9 bit)}} + \underbrace{\text{---}}_{\text{53 Bit representation}} + \underbrace{\underbrace{X}_{\text{Lymphoid (1 bit)}}}_{\text{---}} + \underbrace{\underbrace{X}_{\text{Skeletal (5 bit)}}}_{\text{---}}}_{(1)}$$

where  $X$  is the bit string of length equal to the number of sublevels for that System Name (L1). After encoding the organ selection into bit representation, we send it to the server, where it is decoded and used to render the selected organs.

#### 4.5 Label Information

This functionality enables users to obtain detailed information about a selected organ through a straightforward single-hand gesture. To activate this feature, the user simply needs to form a fist with their right hand while keeping it within the camera's field of view and directing it toward the desired organ as shown in figure 5. Notably, this feature is allowed to be used in conjunction with other functionalities and invoked at any point during the interaction.

#### 4.6 Navigation

This feature enables users to navigate in the AR environment. Instead of adjusting the camera position, which

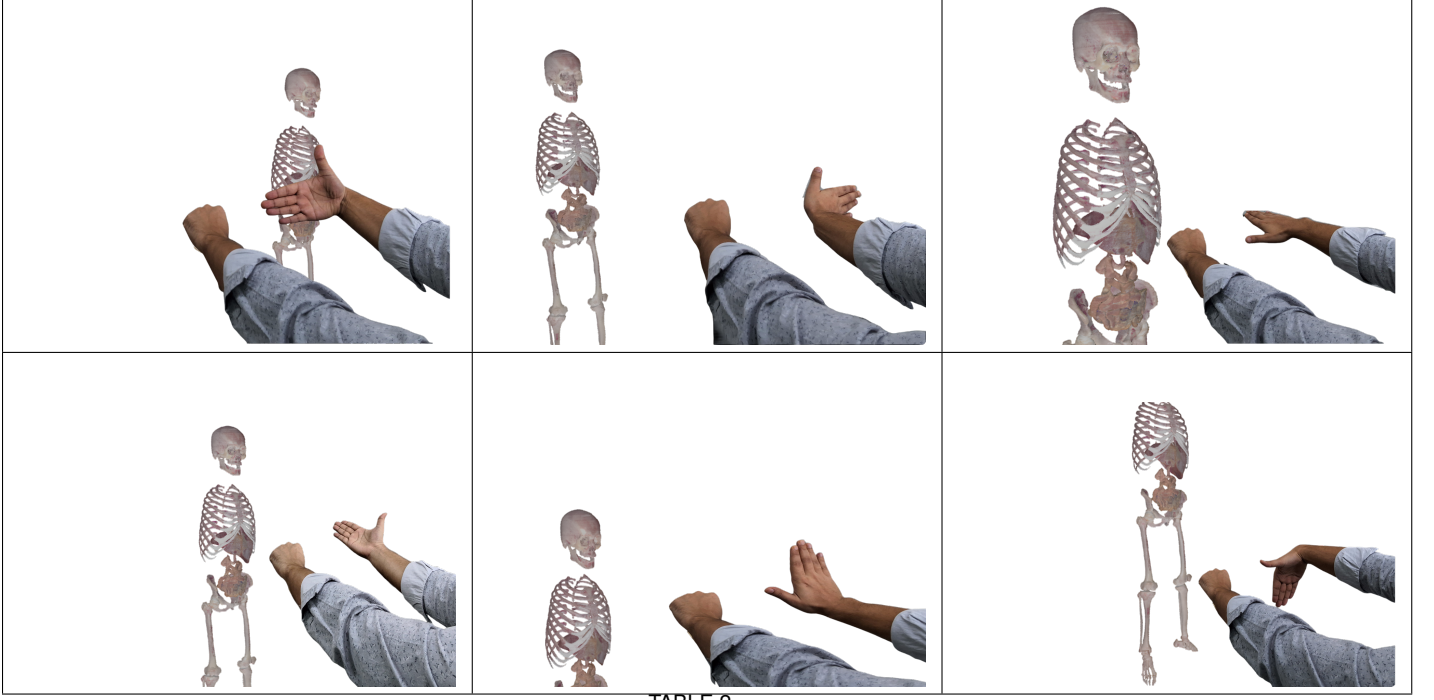


TABLE 2

Navigation gestures, where the right hand represents the camera moving direction. Top row (Left to Right): Moving Left, Moving Right, Moving Forward; Bottom row (Left to Right): Moving Backward, Moving Up, Moving Down.

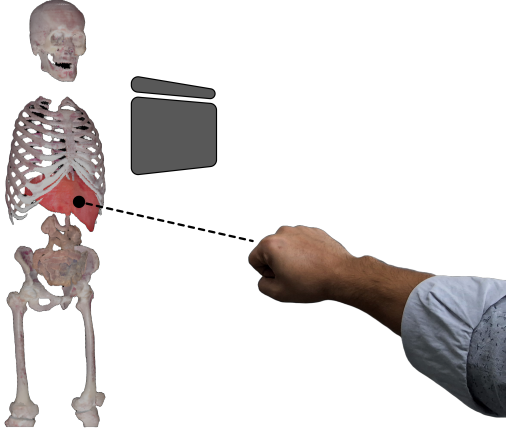


Fig. 5. Label: User points at the organ and makes a fist with the right hand to get the organ information.

remains fixed to the user's head, the system manipulates the position of the body model in the AR world. Navigation is facilitated through a dual-hand interaction mechanism: the right hand determines the direction of movement, while the left-hand serves as a trigger. To activate navigation, the user forms a fist with their left hand, ensuring it remains within the camera's view, while the right hand specifies the desired direction. For directional input, the right hand must be held with the palm straight. Specific gestures for controlling movement are outlined in Table 2.

During navigation, users can get anatomical information via informational labels dynamically attached to the corresponding organs. This interactive approach enhances the

learning experience by combining spatial exploration with contextualized anatomical knowledge.

#### 4.7 Bioscope

A comprehensive understanding of the intricate structural anatomy of every organ and part of the human body is crucial for medical students and professionals. To facilitate this, we developed Bioscope, a feature that enables users to explore anatomical details at an advanced level. Accessing this mode requires the user to perform a specific two-hand gesture. The left hand must be flattened with the palm facing downward, while the right hand executes a pinch gesture directed toward the desired organ shown in figure 6. Upon activation, the selected organ is animated to reposition itself directly in front of the user. At the conclusion of the animation, the organ appears enlarged to twice its original size.

In this mode, users retain access to functionalities such as slicing planes, navigation, and transformations, including translation and rotation. For visualizing the internal structures of organs, we implemented the transfer function based on the gradient of the cryo volume [43]. Additionally, the final voxel opacity is modulated according to equation 2 as published in [44].

$$opacity = o_v \left( k_{gc} + k_{gs} * (\|\nabla \vec{V}_o\|)^{k_{ge}} \right) \quad (2)$$

where  $\nabla \vec{V}_o$  is the normalized color gradient vector,  $k_{gc}$ ,  $k_{gs}$  and  $k_{ge}$  are user defined variables.  $o_v$  is the original intensity values (scalar color component). To reduce the stress on the User, we only provide control over the modulation parameter  $k_{gc}$ , allowing for customization of boundary transparency to enhance visualization clarity.  $k_{gs}$



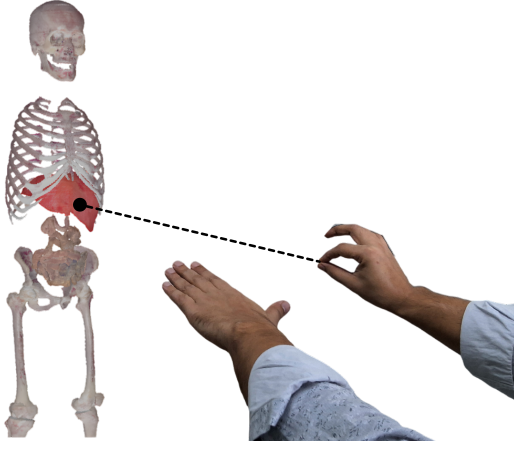


Fig. 6. Bioscope: User points at the organ and makes the pinch gesture with left hand with right palm facing downward to enter into the bioscope mode.

and  $k_{ge}$  are set to 1, and  $o_v$  is set to the average of the RGB components at the voxel.

## 5 RESULTS AND COMPARISON

There are several systems for medical data visualization including MD-Cave [1], VRRRRRoom [25], Nextmed [28], SpatialTouch [2], and 3D Slicer-AR-Bridge [24] that shares conceptual similarities with our proposed system, HoloView, but differ significantly in design, interaction, and application focus.

- 1) *Interaction and User Interface:* HoloView features intuitive, hands-free interaction leveraging hand gestures and eye-tracking, enabling dynamic anatomical exploration. Unlike MD-Cave and VRRRRRoom, which depend on hardware-specific interactions, HoloView eliminates the need for controllers, enhancing accessibility. While SpatialTouch supports multi-device interaction, it lacks the anatomical specificity and refined gesture control of HoloView. Similarly, 3D Slicer-AR-Bridge incorporates AR gestures but does not focus on educational interaction. Nextmed, though effective in automating imaging workflows, does not emphasize user interaction for exploratory learning.
- 2) *Rendering and Performance:* HoloView utilizes GPU-accelerated remote rendering with foveated optimization, ensuring real-time responsiveness even on lightweight AR devices. This contrasts with MD-Cave and VRRRRRoom, which rely on localized rendering infrastructures, and Nextmed, which prioritizes pre-rendered visualization over interactivity. While SpatialTouch and 3D Slicer-AR-Bridge work similarly in utilizing remote rendering but do not implement performance-focused techniques like foveated rendering or hybrid rendering.
- 3) *Hardware and Accessibility:* HoloView can be deployed to lightweight AR devices, making it ideal in varied learning environments. In contrast, MD-Cave requires a dedicated CAVE setup, while VRRRRRoom

depends on desk surface for gesture detection, restricting their flexibility. SpatialTouch's cross-device support introduces versatility but may demand additional hardware, whereas Nextmed and 3D Slicer-AR-Bridge offer moderate portability for clinical use.

- 4) *Application Focus:* HoloView is tailored for medical education, facilitating anatomy learning through features like adjustable transparency, slicing planes, label information, and gesture-driven exploration. MD-Cave and VRRRRRoom cater to radiologists for clinical image analysis, lacking HoloView's pedagogical features. Nextmed and 3D Slicer-AR-Bridge emphasize clinical workflows with a limited focus on interactive exploration. SpatialTouch is not explicitly optimized for medical education. However, it offers a general-purpose approach that applies to various visual domains, including 3D molecular structure data, 3D point cloud data, and 3D anatomical data.

Key features of HoloView, such as integration foveated rendering, intuitive hand gesture controls, and real-time stereo visualization, set it apart from existing systems. By optimizing performance and interaction for anatomy visualization, HoloView bridges the gap between clinical and educational AR applications, ensuring an immersive yet accessible user experience.

## 6 CONCLUSIONS

We developed HoloView, an immersive AR system designed to facilitate the study of human anatomy for medical students. The application leverages foveated rendering, enabled by the eye-tracking capabilities inherent in modern AR devices, to optimize rendering efficiency and enhance the user experience. To eliminate the need for controllers, we implemented intuitive one-hand and two-hand based gesture interactions. A single-hand gesture allows users to access detailed organ information, while two-hand gestures enable navigation within constrained physical environments. The system also includes a bioscope mode, which features a simple slider to adjust the transparency of anatomical boundaries, providing users with an interactive way to explore internal structures.

## ACKNOWLEDGMENTS

This research was supported by the Science and Engineering Research Board (SERB) of the Department of Science and Technology (DST) of India (Grant No. CRG/2020/005792). The Visible Korean Human dataset for our research was provided by the Korea Institute of Science and Technology Information (KISTI), South Korea.

## REFERENCES

- [1] S. Jadhav and A. E. Kaufman, "Md-cave: An immersive visualization workbench for radiologists," *IEEE Transactions on Visualization and Computer Graphics*, vol. 29, no. 12, pp. 4832–4844, 2023.
- [2] L. Zhao, T. Isenberg, F. Xie, H.-N. Liang, and L. Yu, "Spatialtouch: Exploring spatial data visualizations in cross-reality," *IEEE Transactions on Visualization and Computer Graphics*, vol. 31, no. 1, pp. 897–907, 2025.

- [3] M. S. Chung, "Visible korean human. improved serially sectioned images of the entire body," in *2005 IEEE Engineering in Medicine and Biology 27th Annual Conference*, 2005, pp. 6563–6566.
- [4] M. S. Chung, J. Y. Kim, W. S. Hwang, and J. S. Park, "Visible korean human: Another trial for making serially sectioned images," *Proceedings of SPIE - The International Society for Optical Engineering*, 2002.
- [5] —, "Visible korean human: Another trial for making serially sectioned images," *Proceedings of SPIE - The International Society for Optical Engineering*, 2002.
- [6] M. Levoy, "Display of surfaces from volume data," *IEEE Computer Graphics and Applications*, vol. 8, no. 3, pp. 29–37, 1988.
- [7] R. A. Drebin, L. Carpenter, and P. Hanrahan, "Volume rendering," in *Proceedings of the 15th Annual Conference on Computer Graphics and Interactive Techniques*, ser. SIGGRAPH '88. New York, NY, USA: Association for Computing Machinery, 1988, p. 65–74. [Online]. Available: <https://doi.org/10.1145/54852.378484>
- [8] N. Max, "Optical models for direct volume rendering," *IEEE Transactions on Visualization and Computer Graphics*, vol. 1, no. 2, pp. 99–108, 1995.
- [9] D. Laur and P. Hanrahan, "Hierarchical splatting: a progressive refinement algorithm for volume rendering," *SIGGRAPH Comput. Graph.*, vol. 25, no. 4, p. 285–288, jul 1991. [Online]. Available: <https://doi.org/10.1145/127719.122748>
- [10] G. Kindlmann and J. W. Durkin, "Semi-automatic generation of transfer functions for direct volume rendering," in *Proceedings of the 1998 IEEE Symposium on Volume Visualization*, ser. VVS '98. New York, NY, USA: Association for Computing Machinery, 1998, p. 79–86. [Online]. Available: <https://doi.org/10.1145/288126.288167>
- [11] J. Kruger and R. Westermann, "Acceleration techniques for gpu-based volume rendering," in *Proceedings of the 14th IEEE Visualization 2003 (VIS'03)*, ser. VIS '03. USA: IEEE Computer Society, 2003, p. 38.
- [12] T. Kroes, F. H. Post, and C. P. Botha, "Exposure render: An interactive photo-realistic volume rendering framework," *PLoS ONE*, vol. 7, no. 7, 2012. [Online]. Available: <https://doi.org/10.1371/journal.pone.0038586>
- [13] E. Dappa, K. Higashigaito, J. Fornaro, S. Leschka, S. Wildermuth, and H. Alkadhi, "Cinematic rendering – an alternative to volume rendering for 3d computed tomography imaging," *Insights into Imaging*, vol. 7, no. 6, pp. 849–856, 2016. [Online]. Available: <https://doi.org/10.1007/s13244-016-0518-1>
- [14] E. Z. Barsom, M. Graafland, and M. P. Schijven, "Systematic review on the effectiveness of augmented reality applications in medical training," *Surgical Endoscopy*, vol. 30, no. 10, pp. 4174–4183, 2016. [Online]. Available: <https://doi.org/10.1007/s00464-016-4800-6>
- [15] S. Barteit, L. Lanfermann, T. Bärnighausen, F. Neuhaus, and C. Beiersmann, "Augmented, mixed, and virtual reality-based head-mounted devices for medical education: Systematic review," *JMIR Serious Games*, vol. 9, no. 3, p. e29080, Jul 2021. [Online]. Available: <https://doi.org/10.2196/29080>
- [16] M. Ma, P. Fallavollita, I. Seelbach, A. M. Von Der Heide, E. Euler, J. Waschke, and N. Navab, "Personalized augmented reality for anatomy education," *Clinical Anatomy (New York, N.Y.)*, vol. 29, no. 4, pp. 446–453, 2016. [Online]. Available: <https://doi.org/10.1002/ca.22675>
- [17] K. S. Tang, D. L. Cheng, E. Mi, and P. B. Greenberg, "Augmented reality in medical education: a systematic review," *Canadian Medical Education Journal*, vol. 11, no. 1, pp. e81–e96, 2020. [Online]. Available: <https://doi.org/10.36834/cmej.61705>
- [18] C. Moro, J. Birt, Z. Stromberga, C. Phelps, J. Clark, P. Glasziou, and A. M. Scott, "Virtual and augmented reality enhancements to medical and science student physiology and anatomy test performance: A systematic review and meta-analysis," *Anatomical Sciences Education*, vol. 14, no. 3, pp. 368–376, 2021. [Online]. Available: <https://doi.org/10.1002/ase.2049>
- [19] D. Schott, P. Saalfeld, G. Schmidt, F. Joeres, C. Boedecker, F. Huettl, H. Lang, T. Huber, B. Preim, and C. Hansen, "A vr/ar environment for multi-user liver anatomy education," in *2021 IEEE Virtual Reality and 3D User Interfaces (VR)*, 2021, pp. 296–305.
- [20] S. Niedermayr, C. Neuhauser, K. Petkov, K. Engel, and R. Westermann, "Application of 3D Gaussian Splatting for Cinematic Anatomy on Consumer Class Devices," in *Vision, Modeling, and Visualization*, L. Linsen and J. Thies, Eds. The Eurographics Association, 2024.
- [21] R. Metzger, P. Suppa, Z. Li, and A. Vemuri, "Augmented reality navigation systems in endoscopy," *Frontiers in Gastroenterology*, vol. 3, 2024. [Online]. Available: <https://www.frontiersin.org/journals/gastroenterology/articles/10.3389/fgstr.2024.1345466>
- [22] M. Lai, S. Skyman, C. Shan, D. Babic, R. Homan, E. Edström, O. Persson, G. Burström, A. Elmi-Terander, and B. H. W. Hendriks, "Fusion of augmented reality imaging with the endoscopic view for endonasal skull base surgery; a novel application for surgical navigation based on intraoperative cone beam computed tomography and optical tracking," *PLoS ONE*, vol. 15, no. 1, 2020. [Online]. Available: <https://doi.org/10.1371/journal.pone.0227312>
- [23] L. Li, J. Yang, Y. Chu, W. Wu, J. Xue, P. Liang, and L. Chen, "A novel augmented reality navigation system for endoscopic sinus and skull base surgery: A feasibility study," *PLoS ONE*, vol. 11, no. 1, p. e0146996, 2016. [Online]. Available: <https://doi.org/10.1371/journal.pone.0146996>
- [24] H. Li, Y. Yang, Y. Ji, W. Peng, A. Martin-Gomez, W. Yan, L. Qian, H. Ding, Z. Zhao, and G. Wang, "3d slicer-ar-bridge: 3d slicer ar connection for medical image visualization and interaction with ar-hmd," in *2023 IEEE International Symposium on Mixed and Augmented Reality Adjunct (ISMAR-Adjunct)*, 2023, pp. 399–404.
- [25] M. Sousa, D. Mendes, S. Paulo, N. Matela, J. Jorge, and D. S. o. Lopes, "Vrrroom: Virtual reality for radiologists in the reading room," in *Proceedings of the 2017 CHI Conference on Human Factors in Computing Systems*, ser. CHI '17. New York, NY, USA: Association for Computing Machinery, 2017, p. 4057–4062. [Online]. Available: <https://doi.org/10.1145/3025453.3025566>
- [26] J. Taibo and J. A. Iglesias-Guitian, "Immersive 3d medical visualization in virtual reality using stereoscopic volumetric path tracing," in *2024 IEEE Conference Virtual Reality and 3D User Interfaces (VR)*, 2024, pp. 1044–1053.
- [27] C. Lundstrom, T. Rydell, C. Forsell, A. Persson, and A. Ynnerman, "Multi-touch table system for medical visualization: Application to orthopedic surgery planning," *IEEE Transactions on Visualization and Computer Graphics*, vol. 17, no. 12, pp. 1775–1784, 2011.
- [28] S. González Izard, R. Sánchez Torres, O. Alonso Plaza, J. A. Juanes Mendez, and F. J. García-Peñalvo, "Nextmed: automatic imaging segmentation, 3d reconstruction, and 3d model visualization platform using augmented and virtual reality," *Sensors*, vol. 20, no. 10, p. 2962, 2020.
- [29] W. Bethel, "Visapult: A prototype remote and distributed visualization application and framework," 4 2000. [Online]. Available: <https://www.osti.gov/biblio/788012>
- [30] K. Engel, P. Hastreiter, B. Tomandl, K. Eberhardt, and T. Ertl, "Combining local and remote visualization techniques for interactive volume rendering in medical applications," in *Proceedings Visualization 2000. VIS 2000 (Cat. No.00CH37145)*, 2000, pp. 449–452.
- [31] S. Prohaska, A. Hutanu, R. Kahler, and H.-C. Hege, "Interactive exploration of large remote micro-ct scans," in *IEEE Visualization 2004*, 2004, pp. 345–352.
- [32] S. Shi, K. Nahrstedt, and R. Campbell, "View-dependent real-time 3d video compression for mobile devices," in *MM'08 - Proceedings of the 2008 ACM International Conference on Multimedia, with co-located Symposium and Workshops*, ser. MM'08 - Proceedings of the 2008 ACM International Conference on Multimedia, with co-located Symposium and Workshops, 2008, pp. 781–784.
- [33] D. Schmalstieg, "The remote rendering pipeline-managing geometry and bandwidth in distributed virtual environments," Ph.D. dissertation, Schmalstieg, 1997.
- [34] P. Eisert and P. Fechteler, "Low delay streaming of computer graphics," in *2008 15th IEEE International Conference on Image Processing*, 2008, pp. 2704–2707.
- [35] I. Nave, H. David, A. Shani, Y. Tzruya, A. Laikari, P. Eisert, and P. Fechteler, "Games@large graphics streaming architecture," in *2008 IEEE International Symposium on Consumer Electronics*, 2008, pp. 1–4.
- [36] S. Shi and C.-H. Hsu, "A survey of interactive remote rendering systems," *ACM Comput. Surv.*, vol. 47, no. 4, may 2015. [Online]. Available: <https://doi.org/10.1145/2719921>
- [37] V. Kelkkanen, M. Fiedler, D. Lindero, and M. J. Katchabaw, "Synchronous remote rendering for vr," *Int. J. Comput. Games Technol.*, vol. 2021, jan 2021. [Online]. Available: <https://doi.org/10.1155/2021/6676644>
- [38] O. Sharma and F. Anton, "Homotopy-based surface reconstruction



- with application to acoustic signals," *The Visual Computer*, vol. 27, pp. 373–386, 2011.
- [39] G. Taubin, "A signal processing approach to fair surface design," ser. SIGGRAPH '95. New York, NY, USA: Association for Computing Machinery, 1995, p. 351–358. [Online]. Available: <https://doi.org/10.1145/218380.218473>
  - [40] M. Attene and B. Falcidieno, "Remesh: An interactive environment to edit and repair triangle meshes," in *IEEE International Conference on Shape Modeling and Applications 2006 (SMI'06)*, 2006, pp. 41–41.
  - [41] S. G. Parker, J. Bigler, A. Dietrich, H. Friedrich, J. Hoberock, D. Luebke, D. McAllister, M. McGuire, K. Morley, A. Robison, and M. Stich, "Optix: a general purpose ray tracing engine," *ACM Trans. Graph.*, vol. 29, no. 4, jul 2010. [Online]. Available: <https://doi.org/10.1145/1778765.1778803>
  - [42] J. Ye, A. Xie, S. Jabbireddy, Y. Li, X. Yang, and X. Meng, "Rectangular mapping-based foveated rendering," in *2022 IEEE Conference on Virtual Reality and 3D User Interfaces (VR)*, 2022, pp. 756–764.
  - [43] D. Ebert, C. Morris, P. Rheingans, and T. Yoo, "Designing effective transfer functions for volume rendering from photographic volumes," *IEEE Transactions on Visualization and Computer Graphics*, vol. 8, no. 2, pp. 183–197, 2002.
  - [44] C. J. Morris and D. Ebert, "Direct volume rendering of photographic volumes using multi-dimensional color-based transfer functions," ser. VISSYM '02. Goslar, DEU: Eurographics Association, 2002, p. 115–ff.